Published in final edited form as:
J Comp Neurol. 2008 August 10; 509(5): 493–513. doi:10.1002/cne.21757.

Synaptic circuits of the *Drosophila* optic lobe: the input terminals to the medulla

Shin-ya Takemura[1], **Zhiyuan Lu**[1], and **Ian A. Meinerzhagen.**[1,2,3]

[1] Department of Psychology, Life Sciences Centre, Dalhousie University, Halifax, Canada B3H 4J1

[2] Department of Biology, Life Sciences Centre, Dalhousie University, Halifax, Canada B3H 4J1

Abstract

Understanding the visual pathways of the fly's compound eye has been blocked for decades at the second optic neuropile, the medulla, a two-part relay comprising 10 strata (M1–M10), and the largest neuropile in the fly's brain. Based on the modularity of its composition, and two previous reports, on Golgi impregnated cell types (Fischbach and Dittrich, 1989), and their synaptic circuits in the first neuropile, the lamina, we use serial-section EM to examine inputs to the distal strata M1–M6. We report the morphology of the reconstructed medulla terminals of five lamina cells, L1–L5, two photoreceptors, R7 and R8, and three neurons, medulla cell T1, and centrifugal cells C2 and C3. The morphology of these conforms closely to previous reports from Golgi impregnation. This fidelity provides assurance that our reconstructions are complete and accurate. Synapses of these terminals broadly localise to the terminal, and provide contacts to unidentified targets, mostly medulla cells, as well as sites of connection between the terminals themselves. These reveal that: R8 forms contacts upon R7, thus between these two spectral inputs; that L3 provides input upon both pathways, adding an achromatic input; the terminal of L5 reciprocally connects to that of L1, thus being synaptic in the medulla despite lacking synapses in the lamina; that the motion-sensing L1 and L2 lack direct interconnection but both receive input from C2 and C3, resembling lamina connections of these cells; and that, also as in the lamina, T1 provides no output chemical synapses.

Indexing terms

fly; photoreceptors; visual pathway; column; triad; tetrad

Introduction

Studies of neuronal morphology reveal many types of neuron that co-populate a single region of the brain, but usually fail to reveal the connections that actually exist between these neurons. As a result, our knowledge of the synaptic circuits that those connections generate is generally poor and difficult to obtain. Yet the real significance of a neuron's shape lies not in the shape itself, even though this does confer the neuron's cable properties (Jack et al., 1975; Rall et al., 1992), but in bringing that neuron into contact with its targets, and as a result in forming circuits that provide the substrate for behaviour. To elucidate synaptic circuits requires detailed electron microscopic (EM) examinations that are rarely practicable for circuits of any complexity. Only in model structures, such as the retina (e.g.

[3]Corresponding author. I. A. Meinertzhagen, Life Sciences Centre, Dalhousie University, Halifax, Nova Scotia, Canada B3H 4J1, Telephone: (902) 494-2131, Fax: (902) 494-6585, E-Mail: iam@dal.ca.

Dowling, 1987; Sterling, 1998) or cerebellum (e.g. Palay and Chan-Palay, 1974), are clear examples of synaptic circuits known in any detail in the vertebrate nervous system. In most cases these are consensus circuits, based on many cells of the same type, and not necessarily valid for any particular one. The situation is different for certain invertebrate species such as the nematode *C. elegans*, for which an essentially complete wiring diagram has been reported (White et al., 1986), or the fruit fly *Drosophila melanogaster* (referred to here simply as *Drosophila*) in which the availability of genetic tools now warrants the effort required to undertake comparable EM studies, cell by cell. In *Drosophila*, moreover, these same genetic tools begin to provide new methods to dissect the function of synaptic circuits.

The fly's visual system presents what is possibly a unique opportunity for the structural analysis of synaptic circuits. The compound eye comprises an array of ommatidia each with a small, fixed number of cells (26 in *Drosophila*: Ready et al., 1976), of predictable type and combination, containing eight photoreceptor neurons of two main types. Six (R1–R6) terminate in the first optic neuropile, or lamina (Braitenberg, 1967; Strausfeld, 1971; Meinertzhagen, 1976), which is also built on a modular principle, with each module, or cartridge, having a determinate composition. Long visual fibre axons of the other two photoreceptors, the inner photoreceptors R7 and R8, penetrate the lamina (Braitenberg, 1967; Strausfeld, 1971) without synaptic engagements (Boschek, 1971; Meinertzhagen and O'Neil, 1991), and innervate the second neuropile, or medulla.

Each R7 and R8 cell expresses one of two distinct rhodopsins (Morante and Desplan, 2004), and all four subtypes have a distinct spectral sensitivity (Hardie and Kirschfeld, 1983). Pairs of R7 and R8 coordinately express a respective rhodopsin so as to form ommatidia of one of two types and rhodopsin partnerships, called pale and yellow because of their appearance under UV (Franceschini et al., 1981).

These two photoreceptor types establish two systems of input pathway to the medulla (reviewed in Hardie, 1985): 1) Sensory input for high sensitivity vision and motion detection arises from R1–R6; this input is projected indirectly to the medulla by way of lamina cell target neurons, especially L1–L3, possibly as four separate parallel pathways (Bausenwein et al., 1992). 2) Input from R7 and R8 mediates colour discrimination (Heisenberg and Buchner, 1977; Troje, 1993; Pichaud et al., 1999). R7 and R8 innervate the same medulla column that is innervated by the lamina cartridge beneath their ommatidium (Meinertzhagen, 1976). As a result, each column receives both R1–R6 input, via lamina cells, and R7 and R8 input from a single ommatidium.

Many classes of optic lobe neuron, each with a unique morphological signature (~59 types in the medulla of *Drosophila*: Fischbach and Dittrich, 1989), have been reported from Golgi impregnation. Detailed accounts on those in the lamina (in *Drosophila*, 17 cells of 12 different types: Fischbach and Dittrich, 1989) and other related fly species (Strausfeld, 1970, 1971, 1976), provide a basis to recognize different classes of synaptic contacts (Trujillo-Cenóz, 1965; Boschek, 1971; Strausfeld and Campos-Ortega, 1977; Shaw, 1984; Meinertzhagen and O'Neil, 1991; Meinertzhagen and Sorra, 2001) and their possible transmitter phenotype (Hardie, 1989; Sinakevitch and Strausfeld, 2004; Kolodziejczyk et al., 2008). Electrophysiological recordings complement these structural studies in *Calliphora* (Douglass and Strausfeld, 1995, 1996) and *Drosophila* (Zheng et al., 2006). In the deep optic neuropiles of the fly lobula complex, large tangential neurons provide motion-sensitive pathways that project to the protocerebrum (Hausen, 1984). In *Drosophila* the forms of optic lobe cell types are confirmed in the lamina from serial-EM reconstruction (Meinertzhagen and Sorra, 2001) and in the lobula by recent use of the MARCM (Lee and Luo, 1999) and Gal4/UAS (Brand and Perrimon, 1993) systems to target reporter gene expression (Scott et al., 2002; Otsuna and Ito, 2006).

Between the lamina and lobula, the second optic neuropile or medulla, the largest neuropile of the fly's brain (Rein et al., 2002), has so far proved an impenetrable neural jungle (Fig. 1). Despite descriptions of its cell types, and the contributions these make to the 10 strata (M1–M10) of the medulla neuropile (Fischbach and Dittrich, 1989), essentially nothing is known about the arrangement of cells, except that they constitute an array of columns (Campos-Ortega and Strausfeld, 1972). These have been presumed to be determinate in composition, like lamina cartridges but with more than five times the number of elements. Nothing is known about the synaptic circuits established within these different strata, although deoxyglucose studies in *Drosophila* do indicate that the strata segregate different functional pathways (Bausenwein and Dittrich, 1992; Bausenwein et al., 1992). The outer six strata, M1–M6 of the distal medulla, receive inputs from lamina cells (Fischbach and Dittrich, 1989), and these are the subject of the following report.

The lack of synaptic information has not hindered attempts to derive circuit information from light microscopy, by overlapping neuronal profiles to predict how photoreceptors might connect to optic lobe neurons that eventually lead to the fly's optomotor behaviour. Such attempts were first made seriously by Cajal and Sánchez (1915) and have been extended more recently (e.g. Strausfeld and Lee, 1991). These models presume that terminals are large, clubbed and exclusively presynaptic, and dendrites fine, branched and exclusively postsynaptic, that terminals contact dendrites where these overlap in the same neuropile stratum, and that axons lack synaptic engagement. Some of these assumptions are however known to be false for the lamina (Meinertzhagen and O'Neil, 1991) and all will require confirmation by EM for the medulla.

In the lamina, candidate pathways are proposed for lateral inhibition and adaptation (Strausfeld and Campos-Ortega, 1977), and for elementary motion detection (Sinakevitch and Strausfeld, 2004). Despite the complete definition of the synaptic populations (Meinertzhagen and O'Neil, 1991) and their numbers (Meinertzhagen and Sorra, 2001) in the lamina, however, these models suffer from our current lack of knowledge of the synaptic circuits of the same cells in the medulla. Thus only part of the story is known in requisite detail. In an attempt to fill this gap in *Drosophila*, we now report the synaptic inputs to, and connections within, the medulla column. These are provided by the following 10 cells with axons in the lamina, that cross in the chiasma between lamina and medulla neuropiles: R7 and R8; five lamina cells L1–L5; T1, with a soma in the medulla cortex; and two centrifugal cells, C2 and C3, with somata beneath the medulla. The morphologies of these cells in *Drosophila* will be presented later. Details of corresponding cells are given for the housefly *Musca domestica*, here called simply *Musca* (Strausfeld, 1971) and summarized for various fly species (Strausfeld, 1970, 1976). Although these studies provide many interesting comparisons, to avoid introducing species differences, reference to previous studies throughout much of this report will be made mostly to those on *Drosophila*.

Materials and Methods

Serial-section electron microscopy

The heads of adult Oregon R wild-type flies between 3 and 5 days post-eclosion were dissected, immersed in a cacodylate-buffered paraformaldehyde and glutaraldehyde primary fixative, and processed for EM, as previously reported (Meinertzhagen and O'Neil, 1991; Meinertzhagen, 1996). Sections from embedded specimens were cut serially at 60 nm, stained with uranyl acetate and lead citrate and examined at 80kV in a Philips Tecnai 12. The orientation of the sections with respect to the head axes (anterior, dorsal) was preserved by comparing the trapezoid shape of the section with the outline of the embedded head. The distal surface of the medulla was approached gradually after frequent examination of semithin sections. A definitive ultrathin section series was cut from a left eye. The

orientation of the eye was such that the pigment layer at the basement membrane of the retina fell in the middle of the section, and was then adjusted so that its circle remained at the centre and did not go to one edge.

Beneath the lamina neuropile the block was re-orientated as required to ensure that the chiasma fell in the centre of the medulla cortex. When the medulla neuropile first appeared, a series of 672 sections (thus 40μm deep) was cut, which include the six strata of the distal medulla (Fischbach and Dittrich, 1989), with fewer than three sections (0.5%) lost. From 530 of these consecutive sections, images from three columns of the medulla neuropile were captured with a Kodak Megaview II digital camera, using AnalySIS software (SIS GmbH: Münster, Germany). We examined three different columns from one medulla neuropile of the fly. For each column a montage of 3 × 3 was collected at a magnification of 8,200. Each montage was 7.5 MB in size and covered an average area of 17 × 22 μm. To identify which profiles from the same structure to capture from section to section took some experience and required frequent comparisons between digital images.

Consecutive images were aligned *seriatim*, first by cropping in Photoshop, to yield an average image size of 4 MB, and then by using software (sEM Align; Fiala and Harris, 2001 downloaded from http://synapses.bu.edu./) to register three manually selected fiducial marks on each image. Profiles of individual cells were outlined and reconstructed in three dimensions using additional software (Reconstruct; Fiala, 2005 downloaded from http://synapses.bu.edu/tools/history.htm). Synapses, cells and reconstructed profiles were recorded and annotated in Excel. Synaptic vesicle numbers were estimated for the terminals of R7 and R8 from profile counts at several levels, corrected by the Abercrombie formula (1946) for the mean profile diameter measured in Reconstruct, for a section thickness of 60 nm.

Results

Summary of cell types in the distal medulla of Drosophila

Most classes of medulla neurons are columnar, having their axons aligned with the long axis of the medulla columns. Of those seen from selective Golgi impregnation, which are thus liable to underestimate the true numbers, there are 26 reported types of transmedullary (Tm) cell with an additional 4 subtypes; 12 medulla intrinsic (Mi) neurons; 13 TmY cells; and 8 distal medulla (Dm) cells; in aggregate a total of at least 59 types (Fischbach and Dittrich, 1989). Per column, these contribute an estimated total of at least 35 actual cells with somata in the medulla cortex (Meinertzhagen and Sorra, 2001). The distribution of different cell types among individual columns, and thus their combination in any one, is not currently understood, but there are obviously too many for each type to be represented in all columns, so that some must either be hypocolumnar (occupying only alternate or scattered columns), or occupy only certain regions of the medulla eye field. Such inequalities would increase if Golgi impregnation failed to reveal all cell types or if those that it does were multiply represented in each column, even though many may be expected to have only a single representative in each column, like lamina neurons (Fischbach and Dittrich, 1989; Meinertzhagen and O'Neil, 1991).

These medulla cells receive innervation from the following 10 neurons with axons in the lamina: the photoreceptors R7 and R8; lamina cells L1–L5, centrifugal cells C2 and C3, and medulla cell T1, some of which – as we show here – also form synaptic partnerships with each other. These neurons, then, represent those with an identifiable input from (L1–L4) or output to (C2, C3, T1), the lamina; L5 has no significant synaptic engagement in the lamina (Meinertzhagen and O'Neil, 1991).

The segregation between presynaptic and postsynaptic sites, on terminals and dendrites respectively, is not complete -- as it would be for vertebrate neurons (Bodian, 1962). For convenience, we nevertheless refer to the structural specializations within these strata as terminals if they arise from photoreceptors (R7, R8) or lamina neurons (L1–L5), and as dendrites if they arise from medulla neurons (T1, C2, C3) rather than refer to both types of neurite simply as processes.

Organization of the medulla column in cross section

We examined one complete series of serial sections of strata M1–M6 from the outer (distal) medulla and report, cell by cell, the synaptic contacts formed by each of these elements. We chose three areas and traced a single column in each through the entire series. The three areas were from the anterior-ventral (column 1), anterior-dorsal (column 2), and posterior-middle (column 3) edges of a rectangle of the medulla which was about 5 dorsoventral column rows high and about 9 anteroposterior column rows wide (Fig. 2). By comparison, the full area of the retinotopic field is about 32 columns high and wide (Ready et al., 1976). Within the medulla we could not clearly see the edges of the neuropile, which receded in the depth of the block face. However, by comparing low magnification montages like those in Fig. 2 at increasing depths, until the margins of the medulla were visible, we could calculate that column 2 was roughly 5 rows from the dorsal margin of the medulla, while column 3 was about 12 rows from its posterior margin. The rectangle's dorsoventral position would then imply that column 1 was about 10 rows from the medulla's dorsal margin, placing it within the approximately 16 dorsal rows above the position corresponding to the lamina's equator.

Profiles of lamina elements occupied fixed positions within the footprint of the medulla column's cross section. Each column received at least 10 axons that were clear at a level distal to stratum M1 (Fig. 2). At this level, thick processes probably of glial cells surround each column so that we can clearly see the border between columns, but the border becomes unclear at deeper levels. The relative positions of the profiles remained fixed, so that the axons of these elements did not braid their positions, even though in each stratum an axon may have distended into a terminal that surrounded neighbouring elements, and masked its position relative to these, and even though L1–L5, R7 and R8 terminated, one by one, with increasing depth. The axons and terminals of R7 and R8 occupied an antero-medial location in the cross sections of the three columns reconstructed, and this made it hard to detect the position of the equator, which is revealed in the lamina by a double row of R7 and R8 axons (Meinertzhagen and O'Neil, 1991). Consistent with the position of the columns, as calculated above, the pattern of elements seen in the three columns was the same. We did not find a mirror-symmetrical pattern of elements, of the sort reported for lamina cells (Braitenberg, 1967), within the cross-sections of columns 1 and 2, which were separated by the furthest dorsoventral extent (Fig. 2). This suggested that all three columns received innervation from the same side of the equator, which thus appeared to be the dorsal region of the medulla. The pattern of the columns' cross sections was congruent with that in a single previous report on *Musca* (Fig. 4 in Strausfeld and Campos-Ortega, 1972). We did not examine whether the ventral medulla had columns with a mirror symmetrical pattern, like cartridges in the lamina (Braitenberg, 1970).

Organization of the medulla strata

Each lamina neuron terminates in a specific stratum of the distal medulla, as defined by Fischbach and Dittrich (1989). As a result, we can identify that stratum by the proximal and distal borders of each lamina input terminal, especially of L1–L5 (Table 1). Stratum M1 is defined by the distal arborization of L1, and stratum M2 by the extent of L2's arborization. In our series, the axon of T1 cell diverged in two directions in M1 (Fig. 3, Fig. 4B), to give

rise to a cell body and a chiasmal fibre; its arborization mostly overlapped the L2 arborization in stratum M2, which also contained the distal arborization of L4 (Fig. 3, Fig. 4A, B). The distal arborization of L5 and C3 occurred in strata M1 and M2 (Figs. 3–5). The overall thickness of strata M1 and M2 was 11.5–13.5 μm. The border between strata M2 and M3 is given by the proximal end of the L2 terminal, while strata M3 and M4 layers have been defined by the terminals of L3 and L4, respectively (Fischbach and Dittrich 1989). In our series, however, we found that L4 terminated in stratum M5 along with the proximal arborizations of L5 and L1 (Fig. 3, Fig. 4A). We therefore define stratum M4 as the narrow layer between the proximal end of L3 and the distal border of stratum M5. Thus, although six strata are reported (Fischbach and Dittrich, 1989) the depths of the terminals in fact define only five of these clearly. To avoid confusion we will retain the original nomenclature, although we will have little need to refer to M4. The overall thickness of strata M3 and M4 was 6.5–8.5 μm. Stratum M5 is defined by the proximal L1 arborization, and also contained the proximal terminals of L4 and L5 (Figs. 3–5). The thickness of M5 was 5–6 μm. R7 terminated in stratum M6 between the level of the L1 terminal and stratum M7, the serpentine layer (Fig. 3, Fig. 4A, C).

Cell types reconstructed from EM series

The profiles of each cell type contribute the elements of a fixed pattern to the column cross section (Figs. 6 and 7), just as in the lamina cartridge, but unlike the latter were only clear once all elements had been reconstructed and each terminal identified. The profiles of medulla cross-sections were otherwise largely anonymous, and the columnar organisation itself only obvious in the distal strata and M5, especially from the large profiles of L1 and L2.

Photoreceptor terminals R7 and R8—The two central cells of each ommatidium project axons that innervate the distal medulla, where R8 terminates in a distal layer, M3, and R7 projects to the stratum M6 (Fischbach and Dittrich, 1989). Possibly corresponding to the pale and yellow spectral subtypes of R7 and R8, their terminals are each reported to constitute one of two types, short or long (Fischbach and Dittrich, 1989). Even though the morphology of the reconstructed terminals closely resembles those previously reported (Fischbach and Dittrich, 1989), however, the three reconstructed columns provided no evidence for the short and long forms of the terminals and all three terminals of each type terminated at a single stratum (R8: M3; R7: M6). Possibly all R7/R8 axon pairs arose, by chance, from ommatidia of the same type, in which case probably the more numerous yellow type (Cook and Desplan, 2001). Furthermore, we do not provide any evidence for the terminals of R7 and R8 in the dorsal rim area, which have a unique structure and function for detecting the vector of polarized light (Hardie, 1984; Wernet et al., 2003).

The terminals of both R7 and R8 contained numerous small round synaptic vesicles with a mean diameter of 44.45 ± 4.72 (mean ± SD) nm (Fig. 9A), larger than those of R1–R6, which also contain histamine (Pollack and Hofbauer, 1991) but are only 31 nm in diameter (Meinertzhagen and O'Neil, 1991). No other vesicle types were seen, strongly suggesting that these terminals release histamine as a single neurotransmitter. There were an estimated 3,500–4,500 vesicles per terminal in R7 and 5,000–6,000 in R8, of which about 70% were localised to strata M5 and M6 in R7 (Fig. 8). The vesicles were concentrated at several locations of thick parts along the length of the terminals, at sites where the terminal enlarged and contained output synapses, designated by presynaptic T-bar ribbons (Fig. 9A). In addition to synaptic vesicles, small invaginating organelles arose from unidentified glial cell processes (Fig. 9B). These resembled the capitate projections found in the R1–R6 terminals in the lamina (Trujillo-Cenóz, 1965;Stark and Carlson, 1986). They differed from capitate projections in having ellipsoidal rather than spherical heads, which were of smaller

diameter, about 95 nm (Edwards and Meinertzhagen, 2008). Preferring not to introduce a new terminology, we will refer to these as R7/R8 capitate projections.

The axon terminals of R7 and R8 always lay adjacent to each other (Fig. 4C, Fig. 6). Their synaptic connections were distributed over several zones. The R7 terminals had 19–22 presynaptic sites, most localised to stratum M5, and a few in stratum M1 or more distal levels (Fig. 8). The R8 terminals had 35–36 presynaptic sites, distributed in strata M1, M2 and M3 (Fig. 8).

One feature of the outputs of R7 and R8 was that they were not symmetrical. Thus R8 provided input to L1, L5, an unidentified medulla cell, and also to R7 (Fig. 10A, C), in both cases at triads or tetrads, and in neither case were corresponding connections formed by R7. R8's inputs to L1 and L5 were located in stratum M1 while those to R7 were found at a more proximal level, mostly in stratum M3. R7 in turn was presynaptic to unidentified medulla cells. In addition, both terminals received inputs from a common element.

Photoreceptor vesicle size and number

It is not clear why inner and outer photoreceptor terminals should have vesicles of different sizes (44 vs 31 nm, respectively, $p \ll 0.01$; *t*-test) when both are thought to contain the same neurotransmitter. Those of R7 and R8 contain in fact about three times the volume, and thus have perhaps three times the histamine content, of those in R1–R6, which number about 43,000 (Borycz et al., 2005). The difference in vesicle sizes suggests that some details of the clathrin pathway for vesicle endocytosis may differ between the two types of terminal. In R1–R6, vesicle endocytosis is localised to the capitate projections (Fabian-Fine et al., 2003), but whether endocytosis also occurs at the smaller capitate projections in R7 and R8 has yet to be confirmed. Endocytosis at those sites would in that case generate larger synaptic vesicles. The larger vesicle size in R7 and R8, and the larger quantum size that might be expected to result, might offset the lower sensitivity of these photoreceptors, relative to R1–R6, as well as reflect the 12-fold smaller vesicle pool and fewer release sites.

In addition to being different from the synaptic vesicles of R1–R6, the mean of the pooled vesicle diameters in the terminals of R7 and R8 (44 nm) was also larger ($p < 0.01$, *t*-test) than the individual means in the L1–L5 and C2/C3 terminals (in which vesicle diameters ranged from 35–37 nm, see below). The same comparison also yielded a difference for the smaller vesicles in the outer photoreceptor terminals, R1–R6, in the lamina (31.08 ± 2.49 nm: mean ± SD) that was likewise significant ($p < 0.01$, *t*-test). Thus both populations of histaminergic vesicles differed from the vesicles of all other cells, R7/R8's being larger and R1–R6's smaller than those, even though the non-histaminergic vesicles did not differ significantly in diameter from each other and yet had different contents in different cells, glutamate, GABA or acetylcholine (Kolodziejczyk et al., 2008).

Lamina monopolar cell terminals L1–L5—The terminals of lamina monopolar cells identify the strata of the distal medulla. Even though they constitute a single class of lamina neuron, these five cells have different functions. L1–L3 constitute one group, receiving input from R1–R6 at the lamina's photoreceptor tetrads (Meinertzhagen and O'Neil, 1991). There, both L1 and L2, but not necessarily L3, may have the capacity to store vesicular glutamate and thus to use this as a neurotransmitter (Kolodziejczyk et al., 2008). These cells also express phenotypic markers for cholinergic transmission (Yasuyama et al., 1995; Kolodziejczyk et al., 2008). It is thus not clear which neurotransmitter these cells actually release, nor whether this is the same from all three cells, and from all presynaptic sites in each cell. L4 is also qualified both to make and store vesicular acetylcholine, and thus is probably cholinergic (Kolodziejczyk et al., 2008). No transmitter phenotype is reported for L5. Consistent with the possibility that all may liberate the same neurotransmitter, all

mononopolar cell terminals contained populations of small, round, clear vesicles of uniform sizes, with diameters ranging from 32 to 35 nm (see below).

Lamina monopolar cell terminal L1: The terminal of L1 is bistratified, with a bi-lobed terminal arbor in the most superficial medulla stratum, M1, and a deeper clubbed terminal in stratum M5 (Fischbach and Dittrich, 1989) (Fig. 3). The terminal arbor in M5 closely embraced the surface of L5's terminal arbor in the same stratum. The relationships between these two terminals were clear when reconstructions of both terminals were visualized together (Fig. 4A, 5A). The profiles of the L1 arborization were characterized by their rather electron-lucent cytoplasm relative to other lamina cells in the column. They also had characteristic invaginating sheets in both M1 and M5, probably arising from the surrounding glial cells (Fig. 9D). Although the profiles of these sheets appeared superficially like those of the capitate projections in R7 and R8 terminals, thee were in fact not tubular but sheet-like partitions of the terminal, which was otherwise rather undivided. The function of such partitions is not known, but possibly connected to the increased surface to volumne ratio they provide to the terminal. The arborization contained a large number of clear, round synaptic vesicles with a mean diameter of 35.45 ± 3.61 (mean ± SD) nm (Fig. 9C).

The L1 terminals had 87–98 presynaptic sites in total, about 60% located in the distal arborization in stratum M1, and the remaining 40% in stratum M5 (Fig. 8). L1 provided input to L5 at more than 25 contacts; this input was reciprocal (Fig. 10D, E). The synaptic connections of L1 provide inputs to at least two medulla neurons, one of which was also postsynaptic to L5. We presume that these are most of L1's outputs and that many are to Tm cells, but none of the targets is in fact known. In addition, L1 received input from R8 in stratum M1 (Fig. 10A). L1 also provided input to C3 and formed reciprocal contacts with C2 (see Fig. 11).

Lamina monopolar cell terminal L2: The terminal of L2 is a little wider than that of L1, forming a single clubbed arbor beneath that of L1, in stratum M2 (Fischbach and Dittrich, 1989) (Fig. 3). The L2 terminal was not unified like that of L1, but distributed as a series of small lobes, and these did not contain the invaginating partitions that were so diagnostic of the L1 terminal. The L2 terminal contained a diffuse population of clear, round synaptic vesicles with a mean diameter of 35.07 ± 3.89 (mean ± SD) nm. The terminals of L2 formed 88–98 presynaptic sites in stratum M2 (Fig. 8). They were presynaptic upon at least four unidentified medulla neurons (Fig. 9E), of which two neurons have synaptic contacts with L4. These neurons were not postsynaptic to L1, indicating that the L1 and L2 channels are separate. L2 was also postsynaptic to C2 at 4 contacts and to C3 at 10 contacts (Fig. 10B; see also Fig. 11).

Lamina monopolar cell terminal L3: The terminal of L3 formed an arbor in the proximal region of stratum M3 (Fischbach and Dittrich, 1989) (Fig. 3) that spread along the dorso-ventral axis of the column's cross section and extended wider than that of L2. The L3 terminal contained many synaptic vesicles with a mean diameter of 36.20 ± 3.41 (mean ± SD) nm. The terminals of L3 had 40–43 presynaptic sites, most (70–80%) located in stratum M3, but the remainder along the axon in strata M1 and M2 (Fig. 8). Many of the elements postsynaptic to the L3 terminal were thin profiles of unidentified medulla neurons, of which two cells were also postsynaptic to either R7 or R8 (see Fig. 11).

Lamina monopolar cell terminal L4: The terminal of L4 is a spreading arbor in stratum M2, and small terminals in stratum M5 (Fischbach and Dittrich, 1989) (Fig. 3). These did clearly extend deeper than the terminal of L3, however, and unlike a previous report we therefore do not include reference to stratum M4 (Fischbach and Dittrich, 1989). The terminals in M5 contained small, clear synaptic vesicles with a diameter of 35.02 ± 3.26

(mean ± SD) nm. In *Drosophila* these probably contain acetylcholine (Kolodziejczyk et al., 2008).

Although the axon of L4 is bundled together with the axons of the column at the distal level, it moves to one side of the column at deeper levels and extends branches between neighbouring columns (Figs. 4A, 6, 7). The terminals in stratum M5 are interesting. Although these were previously depicted as being two (Fischbach and Dittrich, 1989) there are in fact three branches, as is also true in *Musca* (Strausfeld and Campos-Ortega, 1972, their Fig. 3). The axon lies at one edge of its medulla column in stratum M5 and the terminals arise from short collaterals that penetrate two columns along the +x and −y coordinates (and thus that spread in an anterior direction across the medulla). Given the interpolation of the external chiasma, the retinotopic directions of these collaterals correspond to the posteriorly directed collaterals of this cell in the lamina, in a direction from the retina's front to back.

We found a total of 20–23 presynaptic sites on L4's terminal. These were exclusively localised to the arbors in strata M2 and M5 (Fig. 8). In the medulla, L4 renews a synaptic association with L2 that these cells also have in the lamina (Meinertzhagen and O'Neil, 1991). Both provide input to an unidentified medulla element (Fig. 9E, F, and see also Fig. 11).

Lamina monopolar cell terminal L5: L5 forms a branched arborization in strata M1 and M2, and a compact clump of terminals deeper, in stratum M5 (Fischbach and Dittrich, 1989) (Fig. 3). The arborization and terminals contained a number of synaptic vesicles with a mean diameter of 35.56 ± 3.32 (mean ± SD) nm. These arborizations extended over the surface of the L1 terminal (Figs. 4A, 5A, 6B, 7C). The axon exhibited a characteristic inflection at the border between strata M2 and M3 (Fig. 5A).

We found a total of 56–69 presynaptic sites in strata M1, M2, and M5. In strata M1 and M5, L5 forms reciprocal synaptic connections with L1 (Fig. 10D, E), and the terminals are in turn presynaptic upon unknown cells, probably medulla neurons (see Fig. 11). The inputs from L5 to L1 were found with 5 contacts in stratum M1, and with 5 contacts in stratum M5. Together these synapses resolved the longstanding status of L5 as an orphan, which alone among monopolar cells lacks very clear synapses in the lamina, not only in *Drosophila* (Meinertzhagen and O'Neil, 1991) but also *Musca* (Boschek, 1971). In *Drosophila* at least, we can now view the significance of L5 as a lamina cell not from the contributions it makes to circuits in the lamina but in restricting its synaptic engagements instead to the medulla.

Centrifugal cells C2 and C3: The main axons of C2 and C3 extended centrifugally from the proximal medulla and traveled side by side through the distal medulla (Fig. 4D). C2 formed a branched arborization in stratum M1 and had lateral branches in stratum M5 (Fischbach and Dittrich, 1989) (Fig. 3). The main axon of C3 divides into two at the border between strata M2 and M3, giving rise to a more slender collateral which extended downward along the axons of L1 and L5, and terminated in stratum M5 (Figs. 4D, 5B). Both cells had populations of clear, round synaptic vesicles with a mean diameter of 35.34 ± 3.92 (mean ± SD) nm that probably contain GABA (see below).

We found a total of 24 presynaptic sites in C2 but more than twice this number, 51 presynaptic sites in C3. C2 was presynaptic to L2 at 4 clearly identified sites and both pre- and postsynaptic to L1 at 6 and 5 sites respectively in stratum M1 (see Fig. 5B and Fig. 11). C3 was presynaptic upon L2 at 10 sites, and also to T1 (Fig. 10B), and it was postsynaptic to L1 at 3 sites (see Fig. 5B and Fig. 11). (In addition, C3 could also possibly provide reciprocal input upon L1, at sites where both cells have overlapping terminals in stratum

M1, but we have not found C3 synapses at this level, so this remains uncertain.) C2 and C3 were also presynaptic to unidentified cells, which are probably medulla neurons. Overall, L2 receives numerically strong input from C3 and C2, and L1 provides input to both C2 and C3 that is reciprocal for C2 and possibly so for C3. These connections bear some similarities to those made by the same cells in the lamina, where C2 and C3 are presynaptic to all of L1–L3 (Meinertzhagen and O'Neil, 1999; Meinertzhagen and Sorra, 2001). C3's input to L1 and L2 in the lamina mimics the input it also makes to L2 in the medulla but reciprocates inputs from L1, while C2's input to L1 and L2 mimics this cell's inputs in the medulla. Input from either C cell to L3, mimicking that found in the lamina, has not been seen in the medulla. From evidence in the lamina, both C2 and C3 express GABA and its synthetic enzyme, and thus probably use GABA as a neurotransmitter (Buchner et al., 1988;Sinakevitch et al., 2003;Kolodziejczyk et al., 2008), so that all medulla sites of these cells identified here may release GABA, and thus probably function as sign-reversing synapses.

Medulla cell T1: T1 divides into two in the middle of stratum M1 (Fig. 3A–D), with one axon the linking fibre from the soma in the medulla cortex, and the other arborizing in stratum M2. T1 receives input at dyad synapses from C3, at 7 contacts in stratum M2 mentioned above. By contrast, we found no presynaptic sites, making T1 an anomaly because the lamina connections of the same cell are also exclusively postsynaptic (Meinertzhagen and O'Neil, 1991). The morphological signs we now find for chemical synapses indicate that the same is also true in the medulla, so that from anatomical criteria it is not clear where T1's outputs occur. The cytoplasm contained a few synaptic vesicles, possibly compatible with unconventional release from sites that do not contain a T-bar ribbon. Transmission may of course also occur via gap junctions, which our morphological data do not resolve, and which the size and shape of T1 does not favour, at least in the medulla. Our findings for T1 in the medulla thus prompt a reinvestigation of T1's basket endings in the lamina for evidence of such alternative means of transmission.

Terminal shape, synaptic population and strata

Our sample of medulla terminals was limited to three columns. Few as they are, these are sufficient to allow an initial assessment of the morphological determinacy of each terminal type (Fig. 8). Thus, in all three columns the terminal of R8 disappears at the same depth as that at which the proximal terminal of L1 enlarges. On the other hand, the relative depths of terminals differed between other cells. Thus, the proximal depth of L2's terminal matched closely the depth at which L3's terminal expanded only in column 1, and less so in columns 2 and especially 3. The same was true for the relative depths at which the distal terminal of L1 disappeared and L2's terminal expanded, which defined the M1/M2 border closely in column 3 but not in columns 1 and 2. Despite their solid appearance after Golgi impregnation, when seen in thin sections all expanded terminals in fact had many lobes (Figs. 6 and 7).

Some reconstructed terminals matched the corresponding Golgi impregnate very closely, down to small details of many neurites (Fig. 3). Thus, L3's terminal seen from an anterior view closely resembled the Golgi impregnate reported by Fischbach and Dittrich (1989), even though the latter was from the orthogonal plane, containing the chiasma. The terminals of L1, L2 and L5, were likewise all clearly similar to their counterparts from Golgi impregnation. In other cases the match was less complete. Thus, the R7 terminals in all three columns failed to project as deeply beyond the terminals of L1 and L5 (Figs. 3 and 8) as illustrated for the corresponding Golgi impregnates (Fischbach and Dittrich, 1989). The reason for this difference is not clear but might reflect the difficulty of judging the depth of strata in Golgi preparations. For certain other cells, our reconstructions appear incomplete. Thus C2's proximal terminal extends further laterally in Golgi impregnates than in our

reconstructions, and L4's distal neurites are likewise too sparse (Fig. 3). These cases are both most readily explained by a failure to trace the furthest fine neurites.

By contrast with these indeterminacies, the overall numbers of presynaptic sites for each terminal is fairly closely conserved, with at most a range of 10–22% of the mean for all three columns (Table 2). All three R8 terminals, in particular, had closely similar numbers of presynaptic sites. Despite their similarity, it is possible that not all three columns contained terminals from the R7 and R8 cells of the same type of ommatidium, pale or yellow (Chou et al., 1999), which we still have no way to identify in the medulla. The relative abundance (70%) of yellow ommatidia (Franceschini et al., 1981) would make it likely that at least one column was of this type.

Discussion

We present the first substantive analysis of synaptic contacts in the medulla column of *Drosophila*. Our summary accomplishes two initial objectives. First, it starts to identify the remaining synaptic engagements for cells with synaptic circuits previously identified in the lamina (Meinertzhagen and O'Neil, 1991; Meinertzhagen and Sorra, 2001). As a result, we can now begin to piece together the circuits to which these neurons contribute in the medulla. Second, our study is an entry point to the analysis of the medulla cells themselves, especially the many subtypes of populous transmedulla (Tm) cells (Fischbach and Dittrich, 1989). The complete documentation of these will require much further detailed EM analysis.

To summarise our findings: we identify presynaptic sites at input terminals of R7, R8, and L1–L5, which provide input from the periphery, and for C2 and C3, which provide centrifugal input to the medulla, as well as sites at which most of these terminals and also T1 are postsynaptic in columns of the distal medulla. We also identify synaptic connections between these terminals. These connections help resolve the inputs to different pathways, in particular for colour via R7 and R8 inputs (Morante and Desplan, 2008), and to candidate pathways 1 (the L1 pathway) and 2 (the L2 pathway) for motion detection (Bausenwein et al., 1992; Bausenwein and Fischbach, 1992). Some of these connections could not have been predicted from prior studies, for example in the connections of L5, with L1 and with R8.

The morphologies and classes of neurons

Our 3-D reconstructions provide a third method by which medulla neurons or their inputs have now been visualized. Thus the shapes of Golgi impregnated neurons have already been confirmed by targeted gene expression using the Gal4/UAS system (Morante and Desplan, 2008), and these are now confirmed, in the present study, by serial-EM reconstructions. Although some 3D reconstructions may still be incomplete, the close correspondence between Golgi impregnates and many details of some of our 3-D reconstructions is reassuring, and indicates that significant alterations to the morphology of the neurons does not result from the process of Golgi impregnation itself. Likewise, agreement between 3-D reconstruction images and Golgi profiles confirms that the process of sectioning and then reconstructing in 3-D does not distort the neuron and can capture even fine branches completely. Related discussions have been made for vertebrate neurons, especially from comparisons between Golgi impregnation and 3-D reconstruction images from the retina (for example among subtypes of bipolar cell: Cohen and Sterling, 1990). Related discussions on whether cell classes are continuous or discrete (e.g. Fischbach and Dittrich, 1989; Masland, 2004) are not well addressed by our data, which include only three examples of each reconstructed neuron type. In particular, we are not yet able to distinguish which of the three columns we have reconstructed receives R7 and R8 innervation from pale and which from yellow ommatidia. Two morphological subtypes of such terminals are illustrated by Fischbach and Dittrich (1989), which terminate at somewhat different depths, but our data

do not clearly support this distinction, possibly because all three columns are of the same type.

How strictly are synaptic contacts stratified?

Unlike the lamina, the medulla and deeper lobula neuropiles are all stratified. The strata, 10 in the fly's medulla, yield a texture at the light microscopic level that is characteristic for each insect group, and their number has been highly conserved in different groups (Cajal and Sánchez, 1915). The strata of the external medulla are activated in a stimulus-specific manner, and thus functionally encode the visual world (Bausenwein et al., 1992), so stratum-specific circuits are to be anticipated. Correlated with the denser populations of cells and cell types in the medulla, medulla strata can also be seen as a strategy restricting the possible combinations of terminal-to-dendrite overlaps, and thus the complexity of participants at individual synaptic sites. This strategy requires that terminals be predominantly presynaptic and dendrites predominantly postsynaptic, as presupposed in pathways of information flow derived from the overlap of neuronal profiles (e.g. Cajal and Sánchez, 1915; Strausfeld and Lee, 1991; Bausenwein et al., 1992). There are however clear exceptions to this generalization, which in any case require that we can recognise a terminal simply from its shape. R7 and especially R8 lack a clear terminal and form synapses along their length, in regions that are more axon than terminal, as does L3, which is presynaptic at its axon in M1 and M2 (Fig. 8). Most terminals also receive input, from other terminals as well as from medulla circuits, possibly at feedback synapses, and are thus also not exclusively presynaptic.

Relay pathways versus microcircuits

Relay pathways between the lamina and deep optic neuropiles have already been identified on the basis of terminal-to-dendrite overlaps (e.g. Strausfeld and Lee, 1991; Bausenwein et al., 1992). They include in *Drosophila* four tentative pathways that derive input from R1–R6 synapses in the lamina, sort in the medulla, and are identified with various component cells. Two chief motion detection pathways are: pathway 1, to L1 and thence Mi1 (and C3), to T4 cells; and pathway 2, to L2 and thence Tm1 (Tm14 and Mi8), to T5 cells. Both lobula cells T4 and T5 are then reported to provide input to motion-sensitive lobula plate tangential neurons (Strausfeld, 1984; Bausenwein et al., 1992). Pathway 3 collects inputs in stratum M8 and comprises two further sub-pathways: pathway 3a derives inputs from medulla neurons that arborise in stratum M3, which has greatest overlap with the terminals of L3 and R8; and pathway 3b derives inputs from strata M6 and M4, which has greatest overlap with L4 and R7 (Bausenwein et al., 1992). Thus, divergence at the first synapse, a tetrad synapse from R1–R6 (Meinertzhagen and O'Neil, 1991), establishes input to pathways 1, 2 and 3a, while R8 and R7 are thought to provide input to pathways 3a and 3b, respectively. Pathway 3a and 3b thus both receive mixed spectral inputs, in which R1–R6 input to L3 and, indirectly via L2, to L4 (Meinertzhagen and O'Neil, 1991), is mixed with inputs from R8 and R7.

Missing from this story until now, the actual connections of input terminals to the medulla column (Fig. 11) already provide some support for these four pathways. Thus, L1 and L2, which receive closely matched tetrad input in the lamina (Meinertzhagen and Sorra, 2001), are parallel channels with input to independent target neurons in the medulla, as predicted for pathways 1 and 2. Pathway 3a is supported by L3 input to target neurons of R8, although L3 also provides input to the targets of R7, not predicted for this pathway. Additional analysis of these four pathways, and the extent to which they are an accurate or complete description, will have to await further information on the medulla targets of these and the other inputs to the column.

Two problems face the analysis of pathways derived from terminal-to-dendrite overlaps. The first are the assumptions made about the polarity and locations of synapses based on the shapes of neurites, large clubbed terminals providing exclusive input to fine, branched dendrites, both contributed by axons that lack synapses. Medulla input terminals reveal that faith in these features is unwarranted, at least in detail for particular neurons: axons form synapses, and many terminals are both pre- and postsynaptic. Thus, neuron morphology is only a guide to circuits and their design, which must ultimately be investigated at EM level.

The second is that most if not all synapses identified have multiple postsynaptic elements, frequently triads in lamina cell terminals or tetrads in photoreceptor cell terminals. Synaptic transmission is therefore divergent, providing input to medulla cells that show far greater diversity than the lamina cells that receive R1–R6 input. Adding further complexity, we also find hitherto unsuspected connections among the terminals themselves. Thus circuits previously thought of principally as independent synaptic relays from one neuropile stratum to another, either within the medulla or to other optic neuropiles, are augmented by a wide range of lateral circuits. The latter constitute microcircuits of the sort extensively documented in the lamina (Meinertzhagen and Sorra, 2001) that incorporate two- (feedback, reciprocal) or three-element (serial, feedforward) pathways first clearly identified in visual systems (e.g. Dowling and Boycott, 1966). The exact role played by microcircuits is unclear, and the involvement of multi-element network motifs is wholly unexplored, although widely deployed in biological networks (Milo et al., 2002). Opportunities to identify the electrophysiological responses mediated by these circuits may be rare, and despite the technical possibility of such recordings to identify photoreceptor feedback pathways, even in tiny *Drosophila* cells (Zheng et al., 2006), and parallel studies in larger flies (e.g. Douglass and Strausfeld, 1995), circuit complexity confounds ready analysis with the microelectrode. To interpret those recordings that are possible, detailed EM documentation of synaptic contacts will be essential.

Our study thus begins to confront two issues of resolution. The first is ultrastructural, based on the reality that in a complex neuropile studded with closely-spaced synaptic sites between different combinations of many classes of neurons, EM alone can resolve synaptic organelles. The second is one of circuit design, and the extent to which the synaptic circuits of the medulla are to be seen as a simple chain of relay neurons, as envisaged for the insect visual pathway (Cajal and Sánchez, 1915; Strausfeld, 1984; Strausfeld and Lee, 1991; Bausenwein et al., 1992), or as a network of microcircuits and local interneurons acting via network motifs. While the technical aspects of this study have begun to overcome the first issue, our analysis of the medulla is still very preliminary, and will require further work to resolve the second issue, in particular.

Medulla pathways for vision

Earlier analyses have indicated the existence of pathways for motion that involve R1–R6 input to L1 and L2. That input is carefully balanced at the lamina's many tetrad synapses, in both *Drosophila* (Meinertzhagen and O'Neil, 1991; Meinertzhagen and Sorra, 2001) and *Musca* (Nicol and Meinertzhagen, 1982). The suggestion that L1 and L2 are involved in motion sensing comes from many studies on larger fly species, starting for *Musca* with Braitenberg and Hauser-Holschuh (1972), and is explicit for *Drosophila* (e.g. Bausenwein et al., 1992; Bausenwein and Fischbach, 1992). There are also separate R7/R8 colour-encoding pathways (e.g. Morante and Desplan, 2008). Our findings indicate that the anatomical separation between these two pathways, motion and colour, is not complete, and that R8 provides input to L1 (and L5), while L3 provides input to the targets of R7 and R8. R8 also provides input to R7. Contacts between the terminals of photoreceptor spectral subtypes have also been found in a butterfly's lamina with differences between the pattern of connection between ommatidial types (Takemura and Arikawa, 2006). Several but not all of

these photoreceptors are, in fact, involved in colour discrimination during foraging behaviour (Koshitaka et al., 2008). Although the function of these contacts is not clear, modifying spectral information at the level of the first synapse seems to be important for colour vision. In *Drosophila*, the spectrally distinct information in these two photoreceptor pathways is predicted likewise to be modified at the first synapse, and also by inputs from the R1–R6 pathway through L3 at the second synapse. The exact nature of these interactions must await further definition of synaptic action at these sites, however.

Our results support a segregation between the pathways of L1 and L2. L1 is reciprocally connected to L5 and each provides input to unidentified medulla neurons, while L2 and L4 have inputs to common medulla cells. The two are connected only by the two centrifugal cells C2 and C3. A recent report demonstrates that the L1 and L2 pathways play a crucial role in motion detection, acting either redundantly, in concert, or independently of each other, depending on the contrast of a moving pattern (Rister et al., 2007). C2 and C3's connections form a bi-parallel network motif with L1 and L2 (Milo et al., 2002), which is reciprocal between L1 and C2. As the most obvious pathways between L1 and L2 at this level in the medulla, these circuits could provide a pair of centrifugal pathways by which, according to the visual context, the relative contributions to motion sensing are switched between the L1 and L2 pathways. From current evidence on the neurotransmitter phenotype of L4 (Kolodziejczyk et al., 2008), that switching could be cholinergic. Inputs from C2 and C3 appear not to be entirely symmetrical (being for example stronger from C3 to L2 than from C2), suggesting that each cell may play a subtly different role in this switching.

Various authors (Borst, 2000) have proposed the L1 and L2 pathways as delayed and non-delayed inputs to arrays of correlation-type (Borst and Egelhaaf, 1989) elementary motion detector (EMD) circuits (Reichardt, 1961), and several models by which these neurons may contribute to the arrays have recently been considered (Rister et al., 2007). In the lamina, L1 lacks presynaptic sites whereas L2 provides reciprocal input to L4 (Meinertzhagen and O'Neil, 1991). As in *Musca* (Braitenberg and Debbage, 1974; Strausfeld and Campos-Ortega, 1977), the same L4 contacts other L2 cells in two adjacent posterior cartridges (Meinertzhagen and O'Neil, 1991). We now report that L4's terminal provides a similar pattern of collaterals in the medulla, in a retinotopic direction also corresponding to front-to-back motion across the retina. This pattern could provide a substrate for unidirectional motion detection, as previously proposed for the lamina in *Musca* (Braitenberg and Debbage, 1974; Strausfeld and Campos-Ortega, 1977), and now repeated in the medulla. It is therefore of interest that L4 provides input to one of L2's medulla targets and receives serial input from L2 via another medulla cell (Fig. 11). Identifying these medulla cells and their connections in the medulla is of particular interest for the next step. There are also hypocolumnar and wholly tangential neurons with large dendrites and terminals covering muliple columns. The existence of such neurons is one of the major differences between the lamina and medulla, and will become a progressive challenge in deeper optic neuropiles. Since our current data series include at most 10 medulla columns, it would be difficult to include such neurons in their entirety from cross sections. Alternative strategies such as labelling the neurons and cutting them in longitudinal sections would then be necessary to trace their synapses.

Finally, L3 lacks identified input to the L1 and L2 pathways, providing an independent pathway required for position information in orientation behaviour (Rister et al., 2007), which our findings suggest could act partly via the R7/R8 pathways.

What anatomy cannot reveal

This study identifies the first synaptic pathways in the medulla, as a start to the final documentation of all synaptic connections within a single column. The latter will of course

neither reveal how the medulla processes visual information nor how the fly actually sees. Both of these will require functional analyses, of which genetic dissection methods (e.g. Rister et al., 2007) are accurate at single-cell level, while technically more difficult electrophysiological methods (e.g. Zheng et al., 2006) document individual connections. Detailed knowledge of the anatomical connections will be required to interpret these, and yet additional functional approaches, for an ultimate explanation of the mechanism of fly vision.

We conclude this report with two important provisos. First, we report only synapses so far identified, in full knowledge that many may not yet be included, and that the connections of medulla cells are still too incomplete to include in this account, and are still a major challenge. Second, although the structure of a synapse may be identified, its gain, polarity of transmission (sign-conserving or sign-reversing), and dynamic properties are all without clear structural correlates. The synapses may also be plastic, as some are already known to be in the lamina (reviewed in Meinertzhagen, 2001). Their function may also be the target of neuromodulation. A number of unidentified elements visible in the medulla have large dense-core vesicles, typical of neuromodulatory neurons (reviewed in Langley and Grant, 1997). Thus, information flow within the medulla's synaptic networks, even those we identify here, may in the end be modified by yet additional mechanisms of plasticity and neuromodulation.

Supplementary Material

Refer to Web version on PubMed Central for supplementary material.

Acknowledgments

NIH grant EY-03592 to IAM

This work was supported by NIH grant EY-03592. We thank Matthew Murphey and Satoko Takemura for help with EM reconstructions, and Mr. Harjit Seyan for the Bodian stained preparation in Fig. 1.

References

Abercrombie M. Estimation of nuclear population from microtome sections. Anat Rec. 1946; 94:239–247. [PubMed: 21015608]

Bausenwein B, Fischbach K-F. Activity labeling patterns in the medulla of *Drosophila melanogaster* caused by motion stimuli. Cell Tiss Res. 1992; 270:25–35.

Bausenwein B, Dittrich APM, Fischbach K-F. The optic lobe of *Drosophila melanogaster* II. Sorting of retinotopic pathways in the medulla. Cell Tissue Res. 1992; 267:17–28. [PubMed: 1735111]

Bodian D. The generalized vertebrate neuron. Science. 1962; 137:323–326. [PubMed: 13870420]

Borst A. Models of motion detection. Nat Neurosci. 2000; 3(Suppl):1168. [PubMed: 11127831]

Borst A, Egelhaaf M. Principles of visual motion detection. Trends Neurosci. 1989; 12:297–306. [PubMed: 2475948]

Borycz JA, Borycz J, Kubów A, Kostyleva R, Meinertzhagen IA. Histamine compartments of the *Drosophila* brain with an estimate of the quantum content at the photoreceptor synapse. J Neurophysiol. 2005; 93:1611–1619. [PubMed: 15738275]

Boschek CB. On the fine structure of the peripheral retina and lamina ganglionaris of the fly, *Musca domestica*. Z Zellforsch mikrosk Anat. 1971; 118:369–409. [PubMed: 5566322]

Braitenberg V. Patterns of projection in the visual system of the fly. I. Retina-lamina projections. Exp Brain Res. 1967; 3:271–298. [PubMed: 6030825]

Braitenberg V. Ordnung und Orientierung der Elemente im Sehsystem der Fliege. Kybernetik. 1970; 7:235–242. [PubMed: 4324777]

Braitenberg V, Debbage P. A regular net of reciprocal synapses in the visual system of the fly, *Musca domestica*. J Comp Physiol. 1974; 90:25–31.

Braitenberg V, Hauser-Holschuh H. Patterns of projection in the visual system of the fly II. Quantitative aspects of second order neurons in relation to models of movement perception. Exp Brain Res. 1972; 16:184–209. [PubMed: 4647183]

Brand AH, Perrimon N. Targeted gene expression as a means of altering cell fates and generating dominant phenotypes. Development. 1993; 118:401–415. [PubMed: 8223268]

Buchner E, Bader R, Buchner S, Cox J, Emson PC, Flory E, Heizmann CW, Hemm S, Hofbauer A, Oertel WH. Cell-specific immuno-probes for the brain of normal and mutant *Drosophila melanogaster*. I. Wildtype visual system. Cell Tiss Res. 1988; 253:357–370.

Cajal SR, Sánchez D. Contribución al conocimiento de los centros nerviosos de los insectos. Trab Lab Invest Biol (Madrid). 1915; 13:1–167.

Campos-Ortega, JA.; Strausfeld, NJ. Columns and layers in the second synaptic region of the fly's visual system: The case for two superimposed neuronal architectures. In: Wehner, R., editor. Information processing in the visual systems of arthropods. Springer-Verlag; Berlin, Heidelberg, New York: 1972. p. 31-36.

Chou WH, Huber A, Bentrop J, Schulz S, Schwab K, Chadwell LV, Paulsen R, Britt SG. Patterning of the R7 and R8 photoreceptor cells of *Drosophila*: evidence for induced and default cell-fate specification. Development. 1999; 126:607–616. [PubMed: 9895309]

Cohen E, Sterling P. Demonstration of cell types among cone bipolar neurons of cat retina. Phil Trans Biol Sci. 1990; 330:305–321.

Cook T, Desplan C. Photoreceptor subtype specification: from flies to humans. Semin Cell Dev Biol. 2001; 12:509–18. [PubMed: 11735387]

Douglass JK, Strausfeld NJ. Visual motion detection circuits in flies: Peripheral motion computation by identified small-field retinotopic neurons. J Neurosci. 1995; 15:5596–5611. [PubMed: 7643204]

Douglass JK, Strausfeld NJ. Visual motion detection circuits in flies: Parallel direction- and non-direction-sensitive pathways between medulla and lobula plate. J Neurosci. 1996; 16:4551–4562. [PubMed: 8764644]

Dowling, JE. The Retina. Harvard University Press; Cambridge, MA: 1987.

Dowling JE, Boycott BB. Organization of the primate retina: electron microscopy. Proc Roy Soc Lond B. 1966; 166:80–111. [PubMed: 4382694]

Edwards TN, Meinertzhagen IA. Mistargeting of axon terminals in photoreceptors that mis-express runt in the *Drosophila* eye. J Neurosci. 2008 (submitted).

Fabian-Fine R, Verstreken P, Hiesinger PR, Horne JA, Kostyleva R, Zhou Y, Bellen HJ, Meinertzhagen IA. Endophilin promotes a late step in endocytosis at glial invaginations in *Drosophila* photoreceptor terminals. J Neurosci. 2003; 23:10732–10744. [PubMed: 14627659]

Fiala JC. *Reconstruct*: a free editor for serial section microscopy. J Microsc. 2005; 218:52–61. [PubMed: 15817063]

Fiala JC, Harris KM. Extending unbiased stereology of brain ultrastructure to three-dimensional volumes. J Am Med Inform Assoc. 2001; 8:1–16. [PubMed: 11141509]

Fischbach K-F, Dittrich APM. The optic lobe of *Drosophila melanogaster*. I. A Golgi analysis of wild-type structure. Cell Tissue Res. 1989; 258:441–475.

Franceschini N, Kirschfeld K, Minke B. Fluorescence of photoreceptor cells observed *in vivo*. Science. 1981; 213:1264–1267. [PubMed: 7268434]

Hardie RC. Properties of photoreceptors R7 and R8 in dorsal marginal ommatidia in the compound eyes of *Musca* and *Calliphora*. J Comp Physiol A. 1984; 154:157–165.

Hardie, RC. Functional organization of the fly retina. In: Autrum, H.; Ottoson, D.; Perl, ER.; Schmidt, RF.; Shimazu, H.; Willis, WD., editors. Progress in Sensory Physiology. Vol. 5. New York: Springer-Verlag; 1985. p. 1-79.

Hardie, RC. Neurotransmitters in compound eyes. In: Stavenga, DG.; Hardie, RC., editors. Facets of Vision. Berlin, Heidelberg: Springer-Verlag; 1989. p. 235-256.

Hardie RC, Kirschfeld K. Ultraviolet sensitivity of fly photoreceptor-R7 and photoreceptor-R8 – Evidence for a sensitizing function. Biophys Struct Mech. 1983; 9:171–180.

Hausen, K. The lobula-complex of the fly: Structure, function and significance in visual behavior. In: Ali, MA., editor. Photoreception and Vision in Invertebrates. New York: Plenum Press; 1984. p. 523-559.

Heisenberg M, Buchner E. The role of retinula cell types in visual behaviour of *Drosophila melanogaster*. J Comp Physiol. 1977; 117:127–162.

Jack, JJB.; Noble, D.; Tsien, RW. Electric Current Flow in Excitable Cells. Oxford: Clarendon Press; 1975.

Kolodziejczyk A, Sun X, Meinertzhagen IA, Nässel DR. Glutamate, GABA and acetylcholine signaling components in the lamina of the fly's visual system. PLoS ONE. 2008 resubmitted.

Koshitaka H, Kinoshita M, Vorobyev M, Arikawa K. Tetrachromacy in a butterfly that has eight varieties of spectral receptors. Proc Biol Sci. 2008; 275:947–954. [PubMed: 18230593]

Langley K, Grant NJ. Are exocytosis mechanisms neurotransmitter specific? Neurochem Int. 1997; 31:739–757. [PubMed: 9413835]

Lee T, Luo L. Mosaic analysis with a repressible cell marker for studies of gene function in neuronal morphogenesis. Neuron. 1999; 22:451–461. [PubMed: 10197526]

Masland RH. Neuronal cell types. Curr Biol. 2004; 14:R497–500. [PubMed: 15242626]

Masland RH, Raviola E. Confronting complexity: strategies for understanding the microcircuitry of the retina. Ann Rev Neurosci. 2000; 23:249–284. [PubMed: 10845065]

Meinertzhagen IA. The organization of perpendicular fibre pathways in the insect optic lobe. Phil Trans Roy Soc Lond Ser B. 1976; 274:555–596. [PubMed: 11512]

Meinertzhagen IA. Plasticity in the insect nervous system. Adv Insect Physiol. 2001; 28:84–167.

Meinertzhagen IA, O'Neil SD. The synaptic organization of columnar elements in the lamina of the wild type in *Drosophila melanogaster*. J Comp Neurol. 1991; 305:232–263. [PubMed: 1902848]

Meinertzhagen IA, Sorra KE. Synaptic organisation in the fly's optic lamina: few cells, many synapses and divergent microcircuits. Progr Brain Res. 2001; 131:53–69.

Milo R, Shen-Orr S, Itzkovitz S, Kashtan N, Chklovskii D, Alon U. Network motifs: simple building blocks of complex networks. Science. 2002; 298:824–827. [PubMed: 12399590]

Morante J, Desplan C. Building a projection map for photoreceptor neurons in the *Drosophila* optic lobes. Semin Cell Dev Biol. 2004; 15:137–43. [PubMed: 15036216]

Morante J, Desplan C. The visual circuit in the medulla of *Drosophila*: function in color vision. 2008 Submitted.

Nicol D, Meinertzhagen IA. An analysis of the number and composition of the synaptic populations formed by photoreceptors of the fly. J Comp Neurol. 1982; 207:29–44. [PubMed: 7096637]

Otsuna H, Ito K. Systematic analysis of the visual projection neurons of *Drosophila melanogaster*. I. Lobula-specific pathways. J Comp Neurol. 2006; 497:928–958. [PubMed: 16802334]

Palay, SF.; Chan-Palay, V. Cerebellar Cortex: Cytology and Organization. New York: Springer-Verlag; 1974.

Pichaud F, Briscoe A, Desplan C. Evolution of color vision. Curr Opin Neurobiol. 1999; 9:622–627. [PubMed: 10508742]

Pollack I, Hofbauer A. Histamine-like immunoreactivity in the visual system and brain of *Drosophila melanogaster*. Cell Tiss Res. 1991; 266:391–398.

Rall W, Burke RE, Holmes WR, Jack JJ, Redman SJ, Segev I. Matching dendritic neuron models to experimental data. Physiol Rev. 1992; 72(Suppl):S159–186. [PubMed: 1438585]

Ready DF, Hanson TE, Benzer S. Development of the *Drosophila* retina, a neurocrystalline lattice. Dev Biol. 1976; 53:217–240. [PubMed: 825400]

Reichardt, W. Autocorrelation, a principle for the evaluation of sensory information by the central nervous system. In: Rosenblith, WA., editor. Sensory communication. Cambridge, MA: MIT Press; 1961. p. 303-317.

Rein K, Zöckler M, Mader MT, Grübel C, Heisenberg M. The *Drosophila* standard brain. Curr Biol. 2002; 12:227–231. [PubMed: 11839276]

Rister J, Pauls D, Schnell B, Ting CY, Lee CH, Sinakevitch I, Morante J, Strausfeld NJ, Ito K, Heisenberg M. Dissection of the peripheral motion channel in the visual system of *Drosophila melanogaster*. Neuron. 2007; 56:155–170. [PubMed: 17920022]

Scott EK, Raabe T, Luo L. Structure of the vertical and horizontal system neurons of the lobula plate in *Drosophila*. J Comp Neurol. 2002; 454:470–481. [PubMed: 12455010]

Shaw SR. Early visual processing in insects. J Exp Biol. 1984; 112:225–251. [PubMed: 6392468]

Sinakevitch I, Douglass JK, Scholtz G, Loesel R, Strausfeld NJ. Conserved and convergent organization in the optic lobes of insects and isopods, with reference to other crustacean taxa. J Comp Neurol. 2003; 467:150–172. [PubMed: 14595766]

Sinakevitch I, Strausfeld NJ. Chemical neuroanatomy of the fly's movement detection pathway. J Comp Neurol. 2004; 468:6–23. [PubMed: 14648688]

Stark WS, Carlson SD. Ultrastructure of capitate projections in the optic neuropil of Diptera. Cell Tiss Res. 1986; 246:481–486.

Sterling, P. Retina. In: Shepherd, GM., editor. The Synaptic Organization of the Brain. 4. New York: Oxford University Press; 1998. p. 205-253.

Strausfeld NJ. Golgi studies on insects. Part II: The optic lobes of Diptera. Phil Trans Roy Soc Lond B. 1970; 258:135–223.

Strausfeld NJ. The organization of the insect visual system (light microscopy). I. Projections and arrangements of neurons in the lamina ganglionaris of Diptera. Z Zellforsch. 1971; 121:377–441.

Strausfeld, NJ. Atlas of an Insect Brain. Springer-Verlag; Berlin, Heidelberg: 1976.

Strausfeld, NJ. Functional neuroanatomy of the blowfly's visual system. In: Ali, MA., editor. Photoreception and vision in invertebrates. New York: Plenum; 1984. p. 483-522.

Strausfeld, NJ.; Campos-Ortega, JA. Some interrelationships between the first and second synaptic regions of the fly's (*Musca domestica* L.) visual system. In: Wehner, R., editor. Information Processing in the Visual Systems of Arthropods. Berlin, Heidelberg, New York: Springer-Verlag; 1972. p. 23-30.

Strausfeld NJ, Campos-Ortega JA. Vision in insects: Pathways possibly underlying neural adaptation and lateral inhibition. Science. 1977; 195:894–897. [PubMed: 841315]

Strausfeld NJ, Lee JK. Neuronal basis for parallel visual processing in the fly. Vis Neurosci. 1991; 7:13–33. [PubMed: 1931797]

Takemura SY, Arikawa K. Ommatidial type-specific interphotoreceptor connections in the lamina of the swallowtail butterfly, *Papilio xuthus*. J Comp Neurol. 2006; 494:663–672. [PubMed: 16374804]

Troje N. Spectral categories in the learning behaviour of blowflies. Z Naturforsch C. 1993; 48:96–104.

Trujillo-Cenóz O. Some aspects of the structural organization of the intermediate retina of dipterans. J Ultrastruct Res. 1965; 13:1–33. [PubMed: 5840545]

Wernet MF, Labhart T, Baumann F, Mazzoni EO, Pichaud F, Desplan C. Homothorax switches function of *Drosophila* photoreceptors from color to polarized light sensors. Cell. 2003; 115:267–79. [PubMed: 14636555]

White JG, Southgate E, Thomson JN, Brenner S. The structure of the nervous system of the nematode *Caenorhabditis elegans*. Phil Trans Roy Soc Lond Ser B. 1986; 314:1–340.

Yasuyama K, Kitamoto T, Salvaterra PM. Immunocytochemical study of choline acetyltransferase in *Drosophila melanogaster*: An analysis of cis-regulatory regions controlling expression in the brain of cDNA-transformed flies. J Comp Neurol. 1995; 361:25–37. [PubMed: 8550879]

Zheng L, de Polavieja GG, Wolfram V, Asyali MH, Hardie RC, Juusola M. Feedback network controls photoreceptor output at the layer of first visual synapses in *Drosophila*. J Gen Physiol. 2006; 127:495–510. [PubMed: 16636201]

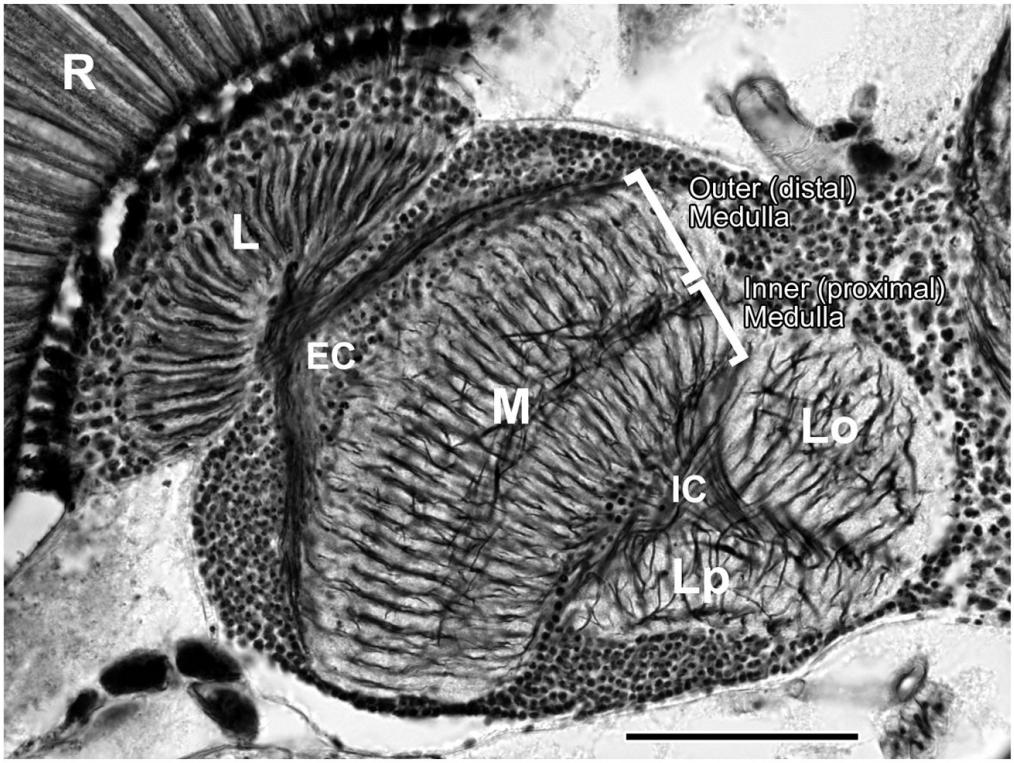

Fig. 1.

Horizontal section of a *Drosophila* visual system from a preparation stained by the Bodian method. Up: direction of the animal's anterior. Horizontal rows of cartridges parallel to the equator in the lamina neuropile (L) connect to horizontal rows of columns in the medulla (M) by means of sheets of fibres that traverse the external chiasma (EC). The medulla is subdivided into two parts, outer (distal, strata M1–M6) and inner (proximal, strata M7–M10), by its middle stratum, which connects to Cuccatti's bundle and contains laterally-orientated axons of many medulla tangential neurons. Each input terminal from the lamina terminates in a specific stratum of the outer (distal) medulla. R, retina; IC, internal chiasma; Lo, lobula; Lp, lobula plate. Scale bar: 50 μm.

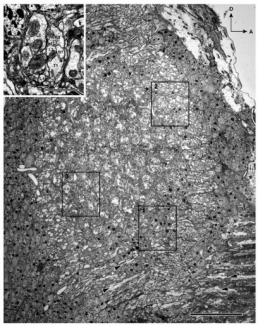

Fig. 2.

Low power montage of a tangential section at a distal level in the medulla neuropile, revealing the three columns (boxes, 1–3) traced through the series from which this image is one section. Sheets of chiasmal fibres (arrowheads) innervate the columns of medulla neuropile. Inset: Column 2 at higher magnification and from a slightly deeper section, illustrating the position of R7 and R8 in this column from the dorsal eye field. Column 2 is separated by 5 dorsoventral column rows from column 1. Dorsal (D) and anterior (A) directions indicate the orientation of the head. Scale bar: 20 μm (inset 2 μm).

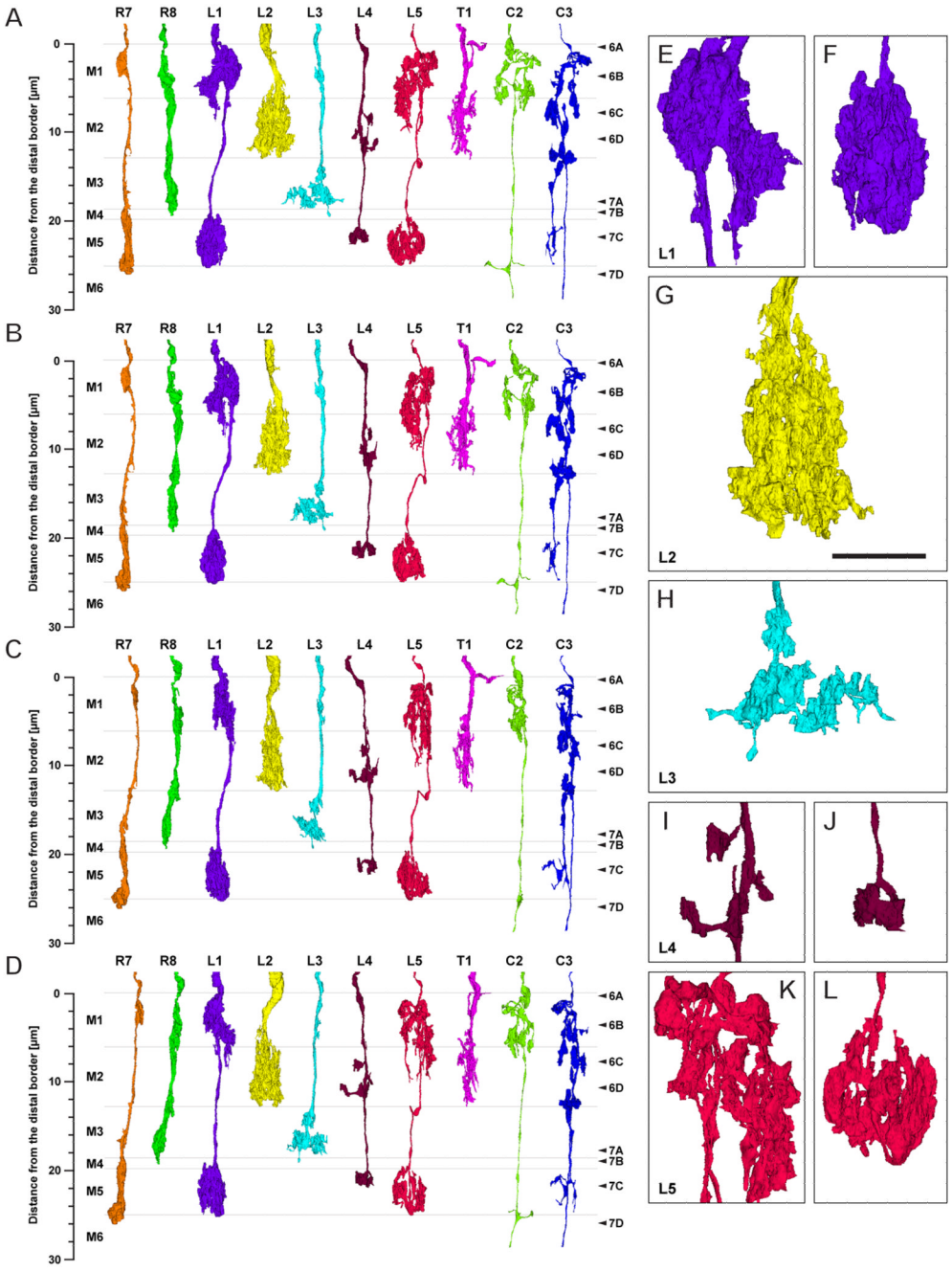

Fig. 3.

Profiles of the 10 cells reconstructed in three dimensions from column 2 in Fig. 2: R7 and R8, L1–L5, C2 and C3, and T1. Because the column is oval in cross section, each cell is shown from four views: from anterior looking posterior (A), in the plane of the chiasma, from dorsal looking ventral (C), and oblique views rotated 45° from the dorsal towards anterior (B) or towards the posterior (D). Borders are indicated between strata M1–M6. Estimated scale of the distance from the distal edge of stratum M1 is shown in the left side. The levels of panels in Figs. 6 and 7 are shown by arrowheads (right side). Enlarged images of terminal arbors of L1–L5 in a posterior view looking anterior (E–L): L1's bi-lobed arbor in stratum M1 (E) and clubbed terminal in stratum M5 (F); L2's terminal arbor in stratum

M2 (G); L3's terminal arbor in stratum M3 (H); L4's spreading arbor in stratum M2 (I) and small terminal in stratum M5 (J); L5's branched arborization in strata M1/M2 (K) and compact clump in stratum M5 (L). Scale bar: 5 μm (in G, same magnification for E–L)

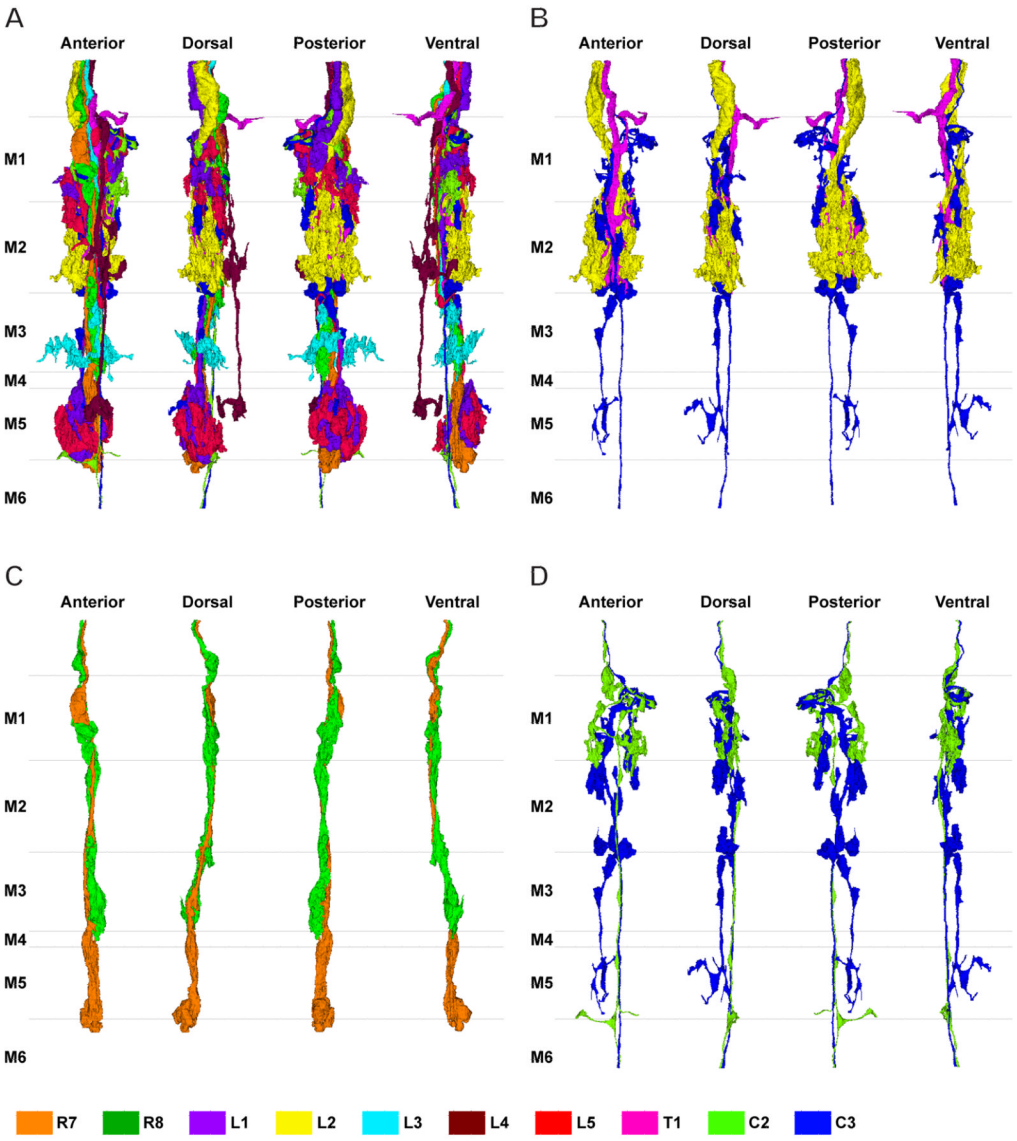

Fig. 4.

Reconstruction of multiple terminals in a single column shown together from four different views at successive 90° rotations in a anticlockwise direction, from the distal surface looking in (far left: view from anterior looking posterior). A: 10 cells reconstructed together. B: C3 (blue) makes contact with L2 (yellow) and T1 (pink) in strata M1 and M2. C: R8 (green) travels with R7 (orange), and is presynaptic to R7. D: The main axon of C2 (yellow-green) and C3 (blue) travel side by side through the medulla within the column.

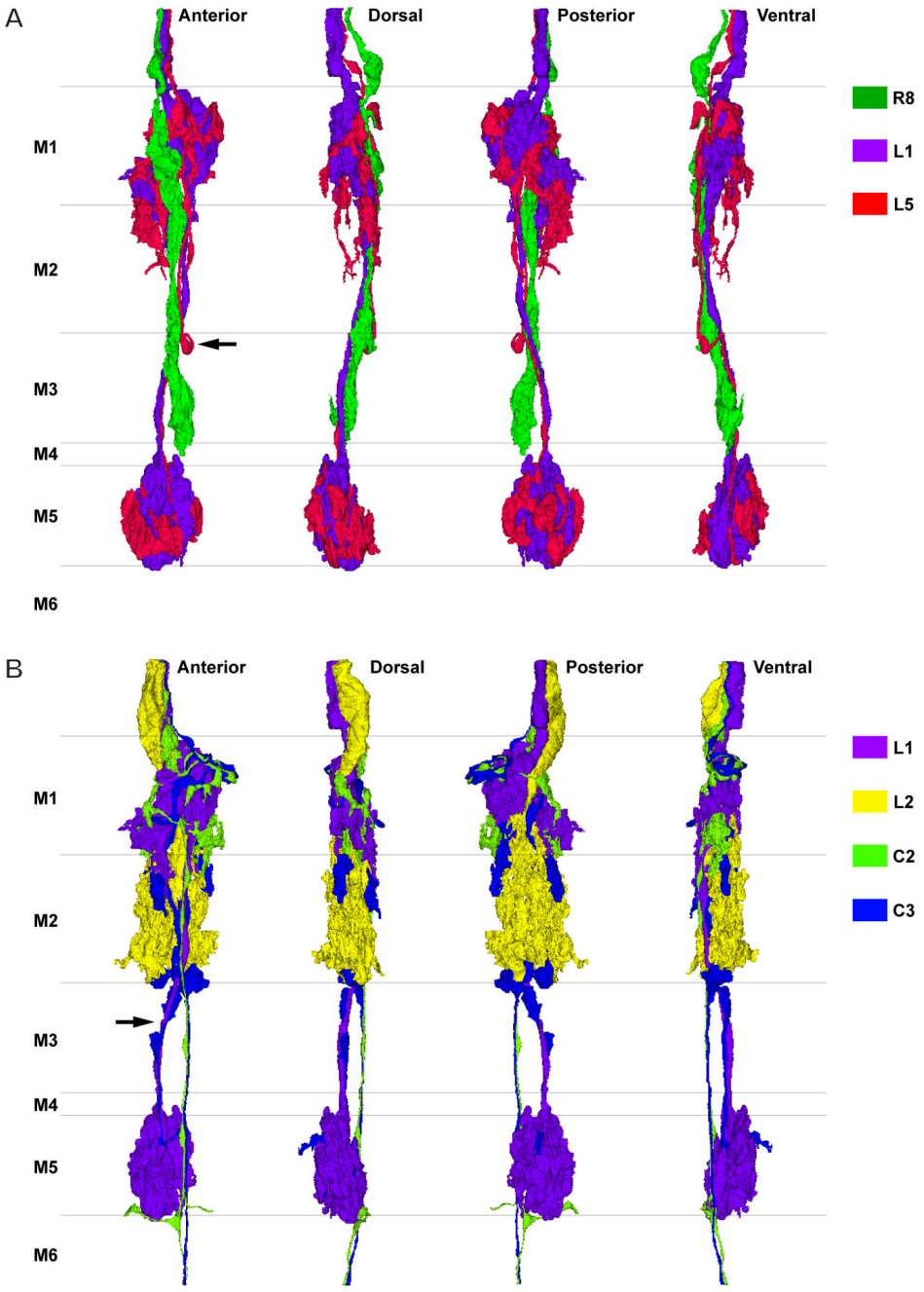

Fig. 5.

A: Reconstruction of the terminals of R8 (green), L1 (purple) and L5 (red). The terminals of L1 and L5 overlap each other closely and have reciprocal synaptic connections in strata M1 and M5. R8 is presynaptic to both L1 and L5 in stratum M1. The axon of L5 has a characteristic inflection around the depth between strata M2 and M3 (arrow). B: Reconstruction of L1 (purple), L2 (yellow), C2 (green), and C3 (blue). C3's short collateral arising from its main axon at the border between strata M2 and M3 travels along the axon of L1 and has synaptic contacts in stratum M5 (arrow). C2 and C3 have numerous synaptic contacts with L1 and L2 (see text for details).

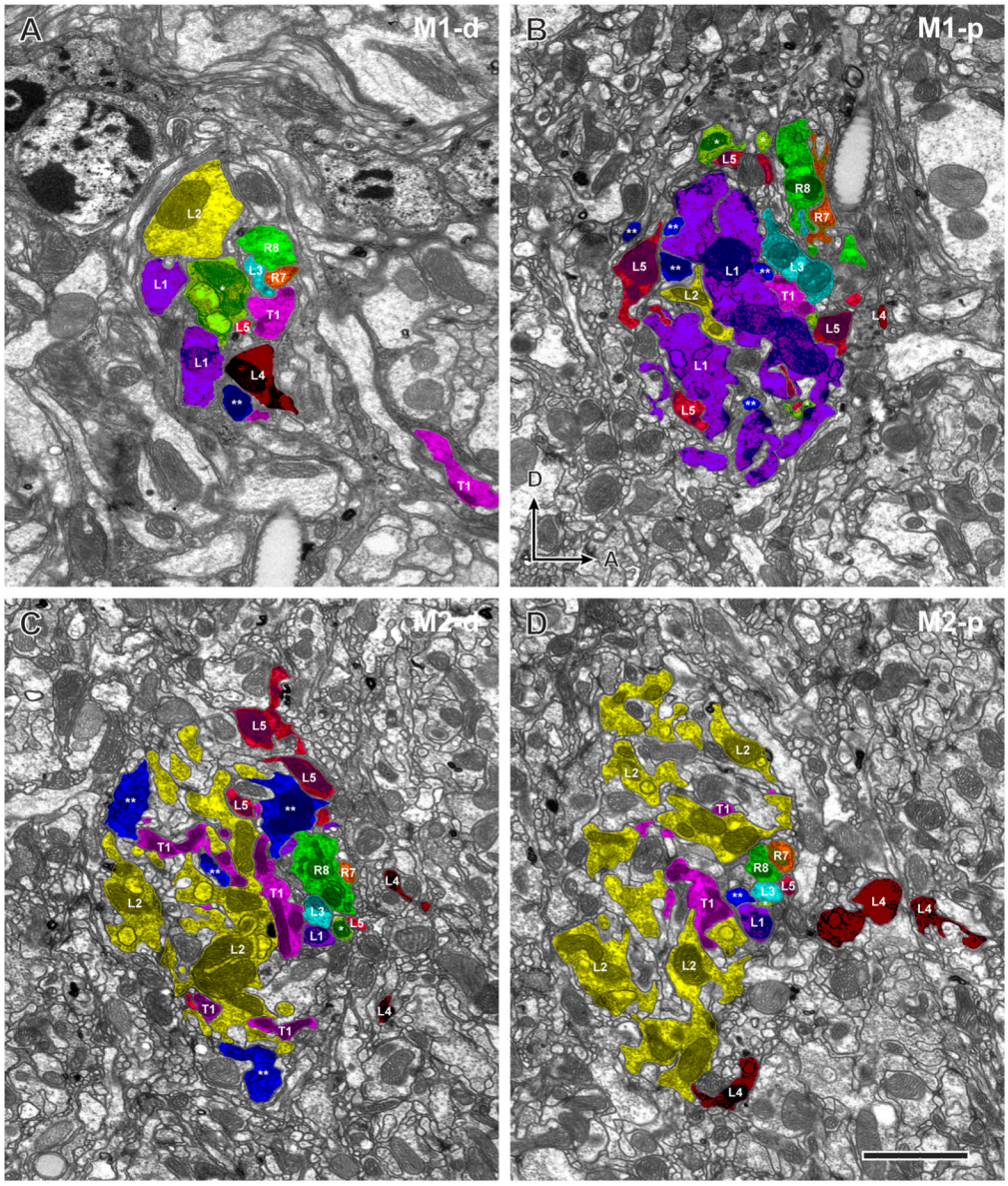

Fig. 6.

Four sections of column 2 from a series of 530 aligned images reveal profiles of all input terminals in the two outermost strata. Profiles of each cell are colour-coded as in Fig. 3, as follows: orange (R7), green (R8), purple (L1), yellow (L2), sky-blue (L3), dark-red (L4), pale-red (L5), yellow-green (C2), blue (C3), and pink (T1). A: Distal region of stratum M1 (M1-d) showing the axon bundle at the chiasma/neuropile border (section no. 73). B: Proximal region of stratum M1 (M1-p) at the level of the expanded terminals of L1 (section no. 123). C: Distal region of stratum M2 (M2-d) at the level of the expanded terminal of L2 (section no. 191). D: Proximal region of stratum M2 (M2-p) containing profiles of the L2 terminal and the divided profiles of the L4 arborization (section no. 240). Dorsal (D) and anterior (A) directions indicate the orientation of the head (in B, for all images). Scale bar: 2 μm (in D, for all images). Micrographs without colour overlays can be found as supplemental figures.

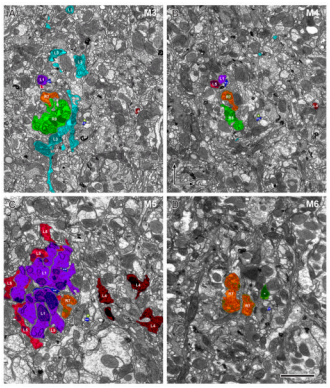

Fig. 7.

Four sections of column 2 in strata M3–M6, continuing those of Fig. 6. A: Stratum M3 containing the spreading terminals of L3 (section no. 347). Note that the dorso-ventrally directed processes of the L3 terminal extend slightly beyond the border of the panel. B: Stratum M4 (section no. 364). C: Stratum M5 at the level of the terminal of L5 and the proximal terminal of L1 showing the three terminals of L4 (section no. 416). D: Stratum M6 at the level of the profiles of the surviving R7 terminal (section no. 479). Dorsal (D) and anterior (A) directions indicate the orientation of the head (in B, for all images). Scale bar: 2 μm (in D, for all images). Micrographs without colour overlays can be found as supplemental figures.

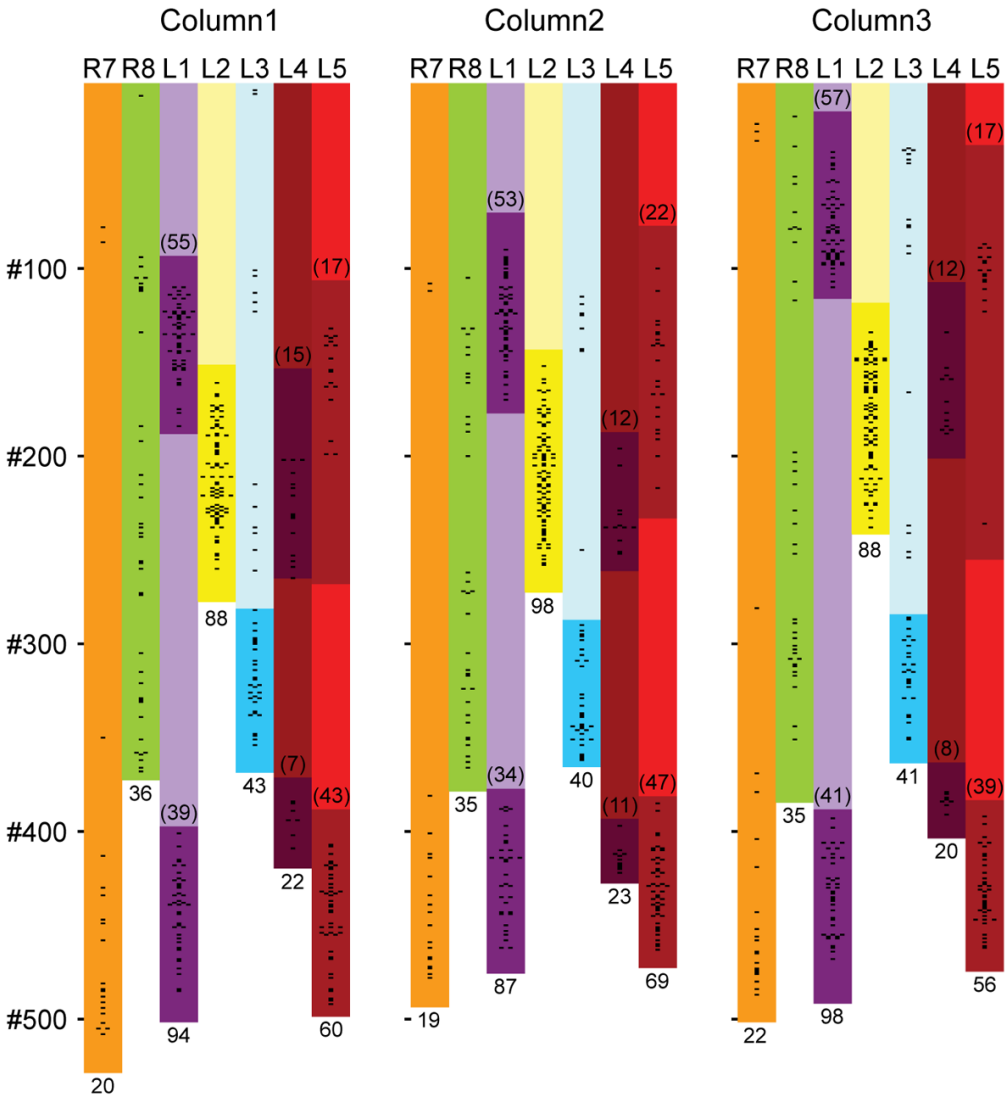

Fig. 8.

Distribution of presynaptic sites along the depths of the terminals of R7 and R8 and L1–L5 in the three reconstructed columns. The profiles of each cell are plotted as a function of section number in the series, from distal (#001) to proximal (#530), and each presynaptic site is indicated by a dot. For each cell (L1–L5), the saturated colour indicates the depth of its expanded terminal. R7 and R8 lack a clear boundary between axon and terminal. The total number of presynaptic sites is shown for each terminal, at the bottom of the bar and, for L1, L4 and L5, above the distal and below the proximal terminal.

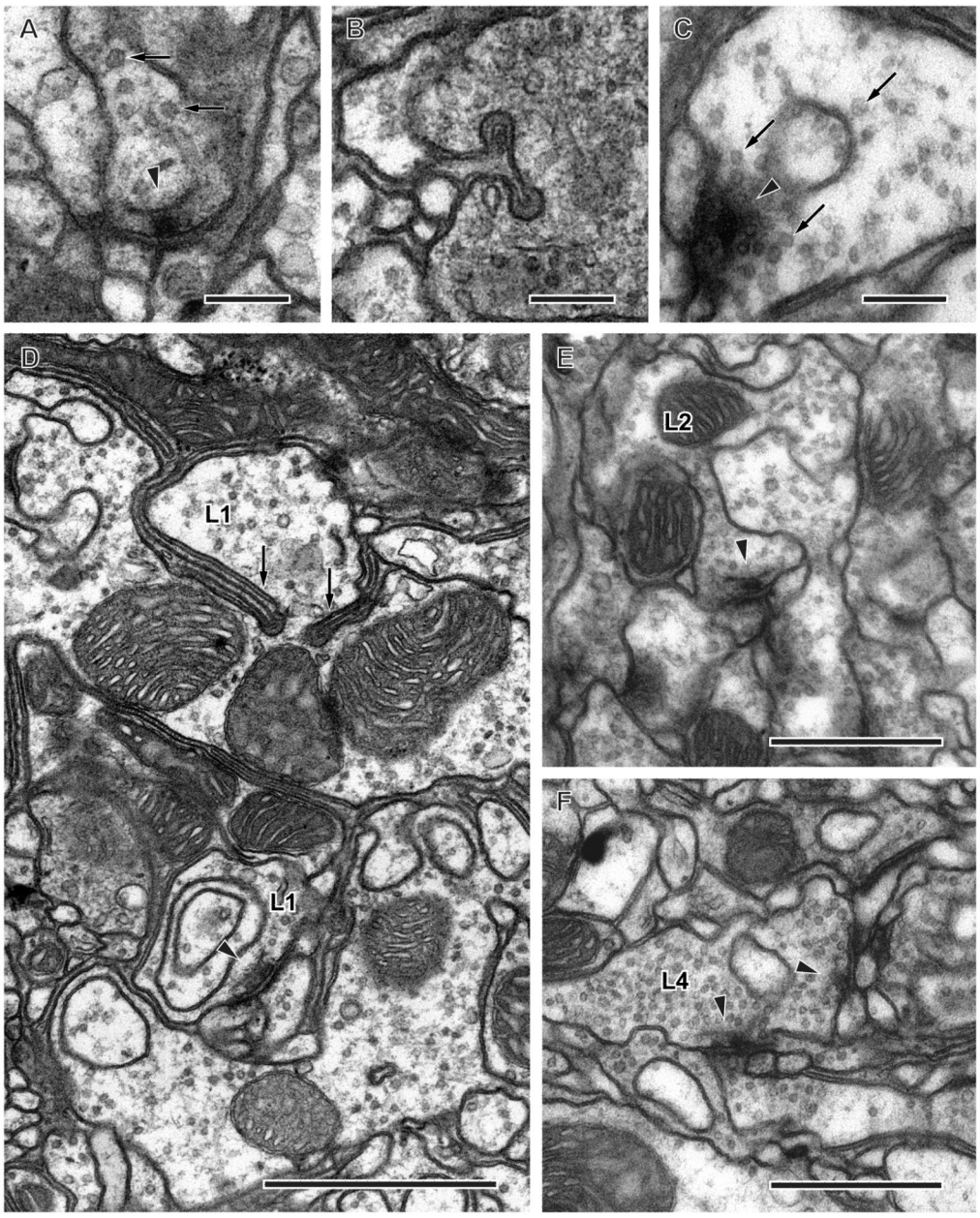

Fig. 9.

Synaptic organelles of photoreceptor and lamina cell terminals in the medulla. A: Presynaptic T-bar ribbon (arrowhead) and synaptic vesicles (arrows) in the photoreceptor terminal R8. B: Invaginating organelle, resembling a capitate projection, in the photoreceptor terminal, arising from an unidentified glial cell. C: Cruciform presynaptic density (arrowhead), the en face view of the pedestal of a T-bar ribbon, and surrounding synaptic vesicles (arrows) in L1 terminal. D: Terminals of L1 have thin invaginating partitions in stratum M5 (arrows). Arrowhead indicates cross-sectioned presynaptic T-bar ribbon in L1 profile. E: L2 is presynaptic to unknown profiles which are probably medulla cells (arrowhead). F: L4 is presynaptic to unidentified profiles which are probably medulla cells in stratum M5 (arrowheads). Scale bars: 0.2 μm (AC); 1 μm (D); 0.5 μm (E, F)

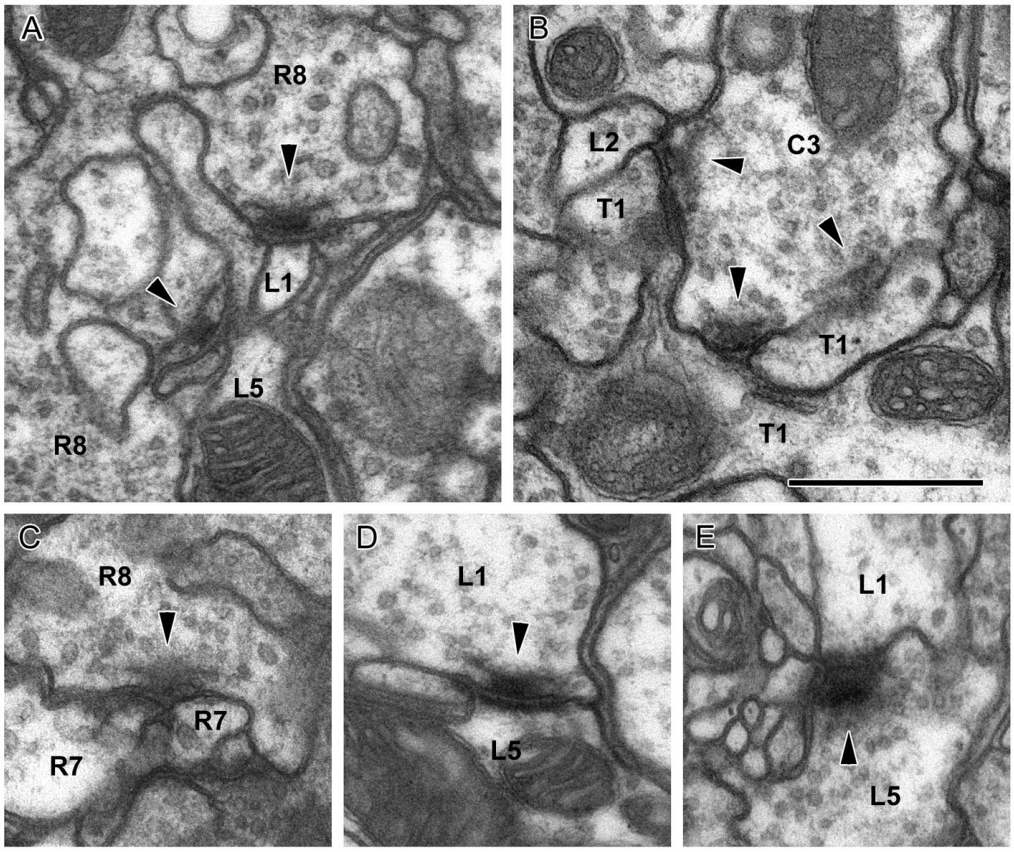

Fig. 10.

Synaptic contacts between input terminals in the medulla column. Arrowheads: T-bar ribbon in presynaptic elements. A: R8 provides input upon L1 and L5. B: C3 provides input upon L2 and T1. C: R8 provides input upon R7 at a dyad. D: L1 provides input upon L5, which is reciprocated at a second site (E). All synapses are of the multiple-contact type and additional postsynaptic elements are not identified. Scale bar: 0.5 μm (in B, for all images).

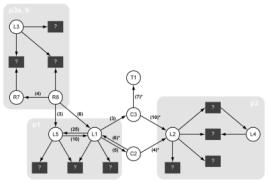

Fig. 11.

Summary diagram of synaptic connections between input terminals to the medulla. The terminals are also presynaptic to many unknown profiles, mostly medulla neurons, that are not yet identified. The numbers of synapses we found in column 2 are indicated by each arrow. The possible neurotransmitter of C2 and C3 (Kolodziejczyk et al., 2008) is GABA (asterisk). Grey shaded panels (p1, p2, p3a,b) represent the previously proposed visual relay pathways (pathway 1, 2, 3a and 3b) of Bausenwein et al. (1992), see text for details). R8 differs from R7 in providing input to L1 and L5, which are themselves reciprocally connected. L1 and L2 have different medulla targets, one of L2's targets also receiving input from L4. L2 receives input from C2 and C3, as it also does in the lamina while, unlike its connections in the lamina, L1 provides input to C2 and C3 that is reciprocal for C2.

Table 1

Strata of the distal medulla and their lamina cell terminals

Stratum					
M1	M2	M3	M4	M5	M6
		R8			
					R7
L1				L1	
	L2				
		L3			
			L4		
L5	L5			L5	
	T1				
C2				C2	
C3	C3			C3	

Data from Fischbach and Dittrich (1989) and Bausenwein et al. (1992)

Table 2

Numbers of pre- and postsynaptic sites at medulla terminals

Cell type	R7	R8	L1	L2	L3	L4	L5
Stratum	M6	M3	M1	M2	M3	M5	M5
			Number of presynaptic sites				
Column 1	20	36	94	88	43	22	60
Column 2	19	35	87	98	40	23	69
Column 3	22	35	98	88	41	20	56
Mean number	20.3	35.3	93.0	91.3	41.3	21.7	61.7
Variation[1]	14.8%	2.8%	11.8%	11.0%	7.3%	13.8%	21.1%
			Number of postsynaptic sites				
Column 2	7	4	14	12	0	1	36

[1] Difference between highest and lowest number, as percentage of mean.

All seven cells were located in all three columns. We had difficulty however to find the processes of remaining cells, especially C2, in all columns. As a result it remains a formal possibility that these cells are not present in all columns.